Available online at www.sciencedirect.com
SCIENCE DIRECT®
Biochemical and Biophysical Research Communications 309 (2003) 232–240
BBRC
www.elsevier.com/locate/ybbrc

Bone-marrow-derived myofibroblasts contribute to the cancer-induced stromal reaction☆

Genichiro Ishii,[a] Takafumi Sangai,[a] Tatsuya Oda,[a] Yasuyuki Aoyagi,[a] Takahiro Hasebe,[a] Naoki Kanomata,[a] Yasushi Endoh,[a] Chie Okumura,[a] Yoko Okuhara,[a] Junji Magae,[b] Makito Emura,[c] Takahiro Ochiya,[d] and Atsushi Ochiai[a,*]

[a] *Pathology Division, National Cancer Center Research Institute East, 6-5-1, Kashiwanoha, Kashiwa-City, Chiba 277-8577, Japan*
[b] *Department of Biotechnology, Institute of Research and Innovation, 1201, Takada, Kashiwa-City, Chiba 277-0861, Japan*
[c] *Institute of Experimental Pathology, Medical School of Hanover, Carl-Neuberg-Str. 1 D-30625, Hanover, Germany*
[d] *Section for Studies on Metastasis, National Cancer Center Research Institute, 1-1, Tsukiji 5-chome, Chuo-ku, Tokyo 104-0045, Japan*

Received 28 July 2003

Abstract

To confirm whether human cancer-induced stromal cells are derived from bone marrow, bone marrow (BM) cells obtained from β-galactosidase transgenic and recombination activating gene 1 (RAG-1) deficient double-mutant mice (H-2b) were transplanted into sublethally irradiated severe combined immunodeficient (SCID) mice (H-2d). The human pancreatic cancer cell line Capan-1 was subcutaneously xenotransplanted into SCID recipients and stromal formation was analyzed on day 14 and on day 28. Immunohistochemical and immunofluorescence studies revealed that BM-derived endothelial cells (X-gal/CD31 or H-2b/CD31 double-positive cells) and myofibroblasts (X-gal/α-smooth muscle actin or H-2b/α-smooth muscle actin double-positive cells) were present within and around the cancer nests. On day 14, the frequencies of BM-derived endothelial cells and BM-derived myofibroblasts were $25.3 \pm 4.4\%$ and $12.7 \pm 9.6\%$, respectively. On day 28, the frequency of BM-derived endothelial cells was $26.7 \pm 9.7\%$, which was similar to the value on day 14. However, the frequency of BM-derived myofibroblasts was significantly higher ($39.8 \pm 17.1\%$) on day 28 than on day 14 ($P < 0.05$). The topoisomerase IIα-positive ratio was $2.2 \pm 1.2\%$ for the H-2b-positive myofibroblasts, as opposed to only $0.3 \pm 0.4\%$ for the H-2b-negative myofibroblasts, significant proliferative activity was observed in the BM-derived myofibroblasts ($P < 0.05$). Our results indicate that BM-derived myofibroblasts become a major component of cancer-induced stromal cells in the later stage of tumor development.

Keywords: Cancer-induced stroma; α-Smooth muscle actin; Desmoplastic reaction; Bone-marrow-derived; Myofibroblast

The invasion of cancer cells into surrounding tissue is the hallmark of malignancy, and the invasion process is associated with considerable destruction and regeneration of intercellular elements, such as the extracellular matrix of the local connective tissue. This newly synthesized stroma is called "cancer induced stroma," and the main constituents of cancer stroma are inflammatory cells, including lymphocytes, granulocytes, and macrophages, the endothelial cells of blood and lymph vessels, pericytes, and fibroblasts. Although roles of inflammatory cells and endothelial cells have been reported to be involved in tumor immunity [1] and neoangiogenesis [2,3], those of fibroblasts which participate in cancer progression have not been fully elucidated yet.

☆ Supported in part by the Grant-in-Aid for Cancer Research (11–12) from the Ministry of Health, Labour and Welfare, the Grant for Scientific Research Expenses for Health Labour and Welfare Programs, the Foundation for the Promotion of Cancer Research, 2nd-Term Comprehensive 10-year Strategy for Cancer Control, and Special Coordination Funds for Promoting Science and Technology from the Ministry of Education, Culture, Sports, Science and Technology, the Japanese Government. T.S. and N.K. are recipients of Research Resident Fellowships from Foundation for Promotion of Cancer Research. M.E. was a Foreign Research Fellow of the Foundation for Promotion of Cancer Research, Tokyo, from October 15, 1998, to March 14, 1999.
* Corresponding author. Fax: +81-471-34-6865.
E-mail address: aochiai@east.ncc.go.jp (A. Ochiai).

0006-291X/$ - see front matter © 2003 Elsevier Inc. All rights reserved.
doi:10.1016/S0006-291X(03)01544-4

Fibroblasts can convert into smooth-muscle-actin-positive fibroblasts, i.e., myofibroblasts or activated fibroblasts, and produce collagens and extracellular matrix proteins in response to several extracellular stimuli [4,5]. This step is called the "desmoplastic reaction" and is a kinetic sequence of events in the invasion process. Investigators of the biology of this cancer-induced stroma, including ourselves have found evidence that the proliferative activity of stromal fibroblasts is closely linked to lymph node and distant organ metastasis [6,7] and that soluble factor secretion by stromal fibroblasts influences tumor progression [8–10]. While most investigators believe that fibroblasts represent a cell type of limited diversity, since fibroblasts have been observed to express subtle biochemical differences and phenotypic variability and to respond differently to cytokines and matrix depending on their tissue origin [11–17], heterogeneity may exist in the biological characteristics of stromal fibroblasts and myofibroblasts. Because of the lack of a good animal model which represents human cancer-induced stroma, the pathogenesis of the stromal reaction in human cancer has remained unclear. In this study, we used human pancreatic cancer cell line Capan-1 that induces desmoplastic stroma when xenotransplanted in severe combined immunodeficient (SCID) mice in order to develop an animal model that would allow analysis of the pathogenesis of the cancer-induced stromal reaction. We used SCID mice as recipients after their bone marrow (BM) cells had been reconstituted with marrow cells from β-galactosidase transgenic and recombination activating gene 1 deficient double-mutant mice. The results showed that the cancer-induced stroma generated by invasive cancer consists of both BM-derived and non-BM-derived myofibroblasts and that BM-derived myofibroblasts were incorporated into cancer induced stroma mainly in advanced stage rather than in early stage of cancer development. This paper reports the first model system for studying the pathogenesis of the cancer-induced stromal reaction by human cancer cells.

Materials and methods

Animals. β-Galactosidase transgenic (β-gal Tg) mice (ROSA 26, C57BL/6 background: H-2b) [18] and recombination activating gene 1 (RAG-1) −/− mice (C57BL/6 background: H-2b) [19] were purchased from Jackson ImmunoResearch Laboratories (West Grove, PA). The β-gal Tg mice were mated with RAG-1−/− mice to generate F1 offspring that were heterogenous for both genes. The F2 offspring of the F1 interbreeding were screened by Western blot analysis for the absence of serum IgM [19]. Mice identified as RAG-1−/− were screened for X-gal staining of peripheral blood mononuclear cells and skin keratinocytes. RAG-1−/− β-gal+/− mice that were identified were further intercrossed, and the F3 offspring were screened based on serum IgM level and X-gal staining level. β-gal Tg and RAG-1−/− mice were further bred in our animal facility. Female SCID mice (C.B-17 background: H-2d), 6 weeks of age, were purchased from CLEA JAPAN, (Tokyo, Japan) and maintained at the National Cancer Center Research Institute East (Chiba, Japan). All animals were maintained under specific-pathogen-free, temperature-controlled-air conditions throughout this study, in accordance with the Institutional Guidelines. Written approval of all animal experiments was obtained from the local Animal Experiments Committee of National cancer Center Research Institute.

Cell preparation and bone marrow transplantation. A 21 G needle on a 5 ml syringe was used to flush bone marrow from the femurs of β-gal Tg RAG-1−/− mice with RPMI-1640 medium. A single cell suspension was prepared by repeated gentle aspirations of the marrow plug with the same syringe and large tissue pieces were removed from the suspension by filtering them through a nylon filter. After 3.5 Gy whole-body irradiation (28 Gy/h) of SCID mice with a 50,000Ci ^{60}Co source in the irradiation room, 1×10^7 donor marrow cells were injected via the tail vein.

Cell staining and analysis. Marrow cells of the SCID recipients were flushed with phosphate-buffered saline (PBS) containing 3% fetal calf serum (FCS), and the suspension was washed and passed through a nylon mesh. Erythrocytes were lysed with ammonium chloride–potassium buffer and the cells were incubated with H-2Kb-FITC (PharMingen, San Diego, CA). After 20 min of incubation on ice, the cells were washed twice and resuspended in PBS supplemented with 3% FCS, 0.02% NaN_3, and 1 mg propidium iodide (PI)/ml. The negative controls were cells stained with isotype-matched mouse immunoglobulin antibodies. Stained cells were analyzed on FACScalibur (Becton–Dickinson, Mountain View, CA).

Cell lines and cell cultures. Human pancreatic cancer cell line, Capan-1 was purchased from American Type Culture Collection (Rockville, MD) and cultured at 37 °C in RPMI 1640 medium containing 20% FCS in a 5% CO_2 incubator.

Capan-1 xenografts in severe combined immunodeficient recipients. At 4 weeks after bone marrow transplantation (BMT), 5×10^6 Capan-1 cells were xenografted into the subcutaneous tissue of SCID recipients. Capan-1 cells were harvested after trypsinization (0.05% trypsin–0.02% EDTA) and collected, washed in medium, counted, and resuspended. Mice were killed by cervical dislocation 2 and 4 weeks after xenografting.

X-gal staining, immunohistochemistry, and immunofluorescence analysis. X-gal staining was performed as previously described [20]. Xenografted cancer tissue was fixed in 4% paraformaldehyde in PBS for 1 h on ice. Fixed samples were washed twice in washing buffer A (PBS containing 2 mM $MgCl_2$–$6H_2O$, and 5 mM EGTA) and washing buffer B (PBS containing 2 mM $MgCl_2$–$6H_2O$, 0.01% sodium deoxycholate, 0.02% Nonidet P-40). After staining samples overnight at 37 °C in X-gal staining solution (0.1% 5-bromo-4-chloro-3-indoyl-β-D-galactopyranosidase, 5 mM $K_3Fe(CN)_6$, and 5 mM $K_4Fe(CN)_6$ in washing buffer B), they were snap frozen, and serial 6 μm sections were counterstained with hematoxylin prior to microscopic examination. Immunohistochemical staining was performed with DAKO EnVision + System-HRP (Dako, Grostrup, Denmark). Samples were prefixed in 4% paraformaldehyde in PBS for 1 h on ice, then washed in washing buffer A and B. The tissues were embedded in OCT compound and snap-frozen in liquid nitrogen. Samples were sectioned at 5-μm and incubated with primary antibodies. The primary antibodies used here were a mouse monoclonal antimouse H-2Kb (AF6-88.5; PharMingen), at a 1:100 dilution; a mouse monoclonal anti α-smooth muscle actin (α-SMA) (1A4; Sigma Chemical, St. Louis, MO), at a 1:400 dilution; a rat monoclonal antimouse CD31(MEC13.3; PharMingen), at a 1:100 dilution, and a rabbit polyclonal anti-topoisomerase IIα (Novocastra, UK), at a 1:100 dilution. Immunofluorescence analysis was performed by sectioning prefixed specimens at 10 μm and incubating them with primary antibodies, including mouse monoclonal antimouse H-2Kb-FITC (AF6-88.5; PharMingen), at a 1:100 dilution; a mouse monoclonal anti α-SMA-Cy3 (1A4; Sigma), at a 1:400 dilution; and a mouse monoclonal anti Vimentin (VIM 3B4; PROGEN, Germany), at a 1:100 dilution. After mounting, sections were examined with MRC-1024 confocal imaging system (Bio-Rad, Gercules, CA). Confocal images were stored as digital files and viewed with Photoshop (Adobe, Mountain View, CA).

Assessment of the immunohistochemistry findings. The proportions of bone marrow-derived endothelial cells were determined by the ratio of H-2Kb positive endothelial cells to the total number of CD31 positive endothelial cells using serial sections. The proportions of bone marrow-derived myofibroblasts were determined by the ratio of H-2Kb positive myofibroblasts to the total number of α-SMA positive myofibroblasts using serial sections. The fields for cell counting were selected in both inner area and outer area of each xenografts ($n = 4$). At least 50 endothelial cells and 100 myofibroblasts were counted in high-power field (400×) and each numerical value was averaged.

Results

Generation of an animal model of the cancer-induced stromal reaction

Sublethally irradiated SCID (H-2d) mice were injected with 1×10^7 BM cells from β-gal Tg and RAG-1 deficient double-mutant mice (β-gal Tg RAG-1−/−, H-2b). H-2 phenotyping of BM cells from the recipient mice demonstrated that their marrows had been reconstituted by high levels (>90%) of donor cells 4 weeks after BMT (Fig. 1). Histological examination did not reveal any obvious evidences of graft-versus-host disease (GVHD) effects in the liver, lungs, colon, skin, or spleen of a large series of SCID recipients. Four weeks after BMT, we subcutaneously inoculated SCID recipients with human pancreatic cancer cell line Capan-1 and 2 and 4 weeks later tumors that had developed were resected and examined histologically. Examination of subcutaneous Capan-1 tumors showed glandular formation with mucus production. Many spindle-shaped fibroblasts were arranged in disarray fashion and intermingled with inflammatory cells in the peritumoral and intratumoral area (Figs. 2A and B). The morphological features of Capan-1 resembled the desmoplastic reaction usually seen in human invasive cancer stroma.

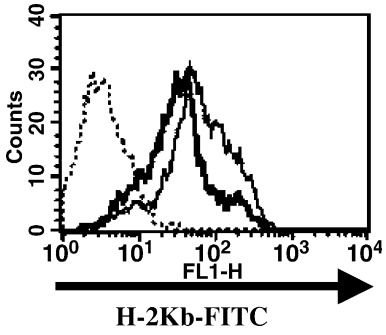

Fig. 1. H-2 phenotyping of BM cells from reconstituted SCID mice. BM cells from the SCID recipient reconstituted by β-gal Tg RAG-1−/− mice were analyzed for H-2Kb expression by flow cytometry (thin line). Marrow cells from SCID mice were used as a negative control (broken line) and cells from donor mice (β-gal Tg RAG-1−/−) were used as a positive control (bold line).

Incorporation of bone-marrow-derived cells into cancer-induced stroma

In order to determine whether BM cells contribute to the pathogenesis of cancer-induced stromal reaction in this model, we first analyzed β-gal enzyme activity in the resected tumors. Fig. 3A shows macroscopic appearance of X-gal whole-mount staining of resected tumors in SCID mice recipients on day 28. The cut surface of the tumors revealed extensive blue areas, whereas the tumors of the SCID mice whose BM was reconstituted with β-gal−/− (wt) RAG-1−/− marrow cells were tanish-white. Microscopically, X-gal-positive cells were found in cancer-induced stroma of SCID mice recipients, whereas no X-gal-positive cells could be detected in the mice reconstituted with β-gal−/− (wt) RAG-1−/− (Figs. 3B and C). The β-gal expressing cells consisted of inflammatory cells, spindle cells, and endothelial cells. These results indicated that donor BM cells were frequently incorporated into cancer-induced stroma. Consistent with previous reports, some endothelial cells were

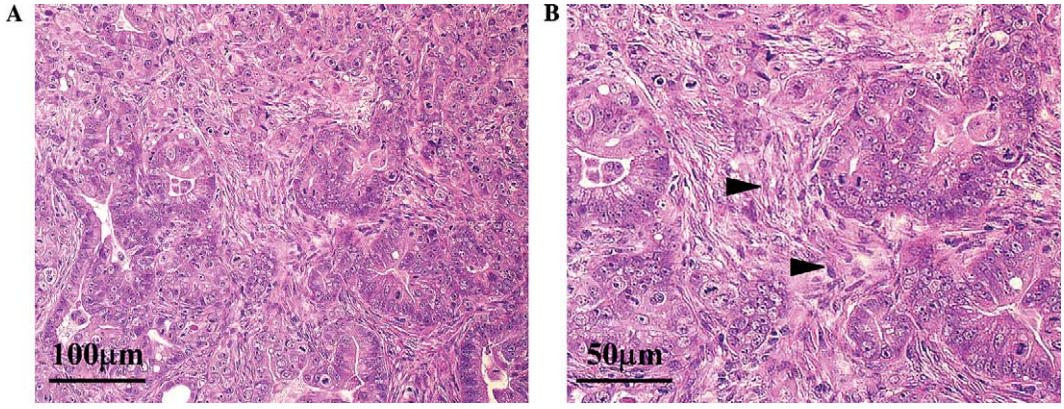

Fig. 2. Microscopic appearance of Capan-1 xenotransplanted into the SCID recipients (day 28). (A) Many spindle-shaped fibroblasts are arranged in disarray fashion and intermingled with inflammatory cells in the peritumoral and intratumoral area. (B) A higher power view of the same area. Stromal formation resembled human desmoplastic stroma induced by invasive cancer. Arrowheads indicate the activated fibroblasts.

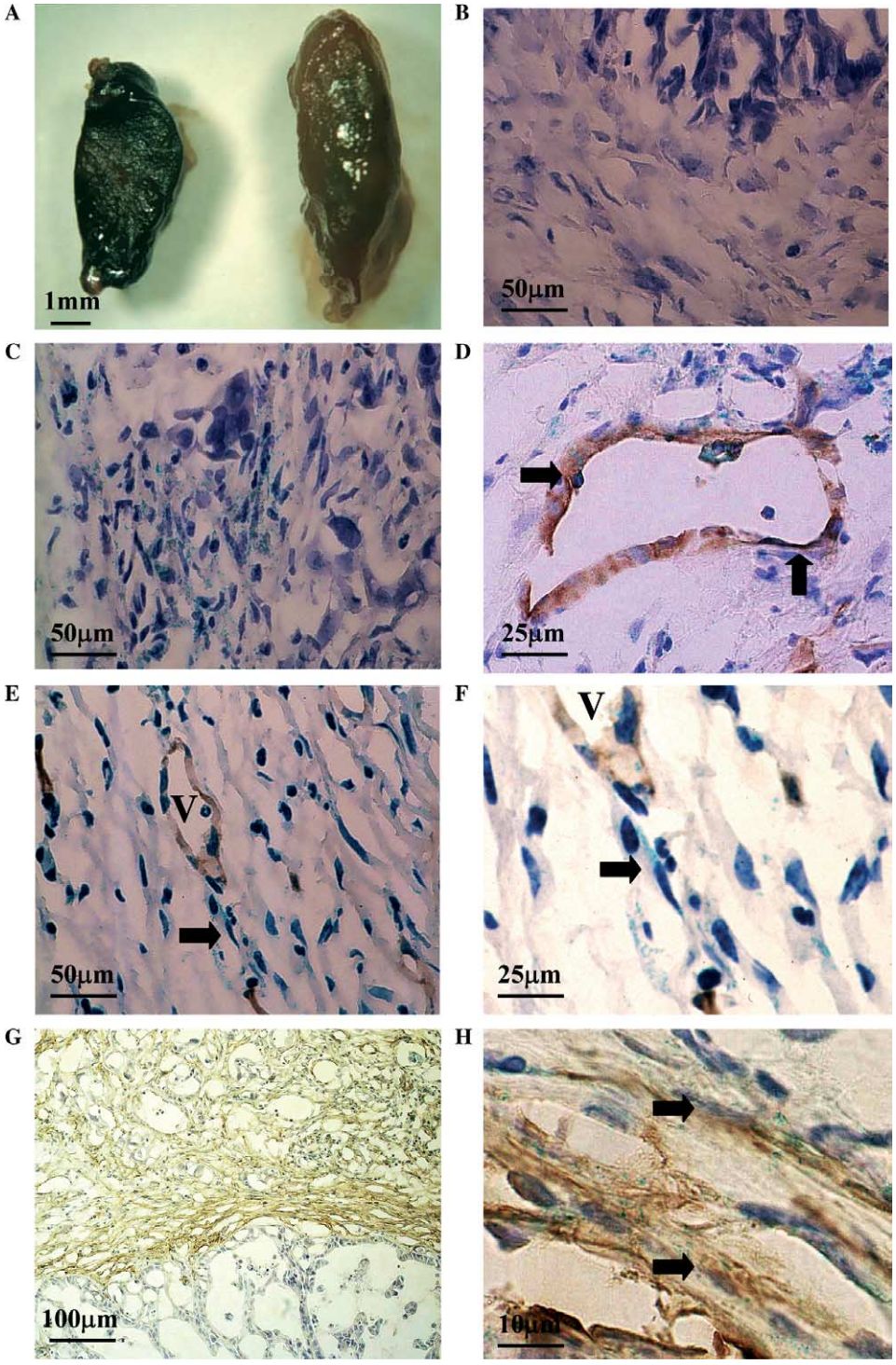

Fig. 3. Detection of donor-BM-derived cells by X-gal staining. (A) Macroscopic appearance of tumors on day 28 after X-gal staining. The cut surface of the tumor of a SCID recipient revealed extensive blue areas (left), whereas the tumor of SCID mice whose BM was reconstituted with the marrow cells of β-gal−/− (wt) RAG-1−/− was tanish-white (right). Microscopic appearance of tumors on day 28 after X-gal staining. No X-gal-positive cells were detected in the tumors of SCID mice whose BM was reconstituted with marrow cells of β-gal−/− (wt) RAG-1−/− mice (B). X-gal-positive cells were found in cancer desmoplastic stroma of SCID recipients whose BM was reconstituted with the marrow cells of β-gal Tg RAG-1−/− mice (C). Some endothelial cells were X-gal/CD31 double-positive (*arrow*, D). Spindle cells that were unassociated with vasculature and reacted positively for X-gal were observed (*arrows*, (E). High-power photograph of E (F). Spindle cells within and around the cancer nest were α-SMA positive (G). These myofibroblasts were both α-SMA- and X-gal-positive (H).

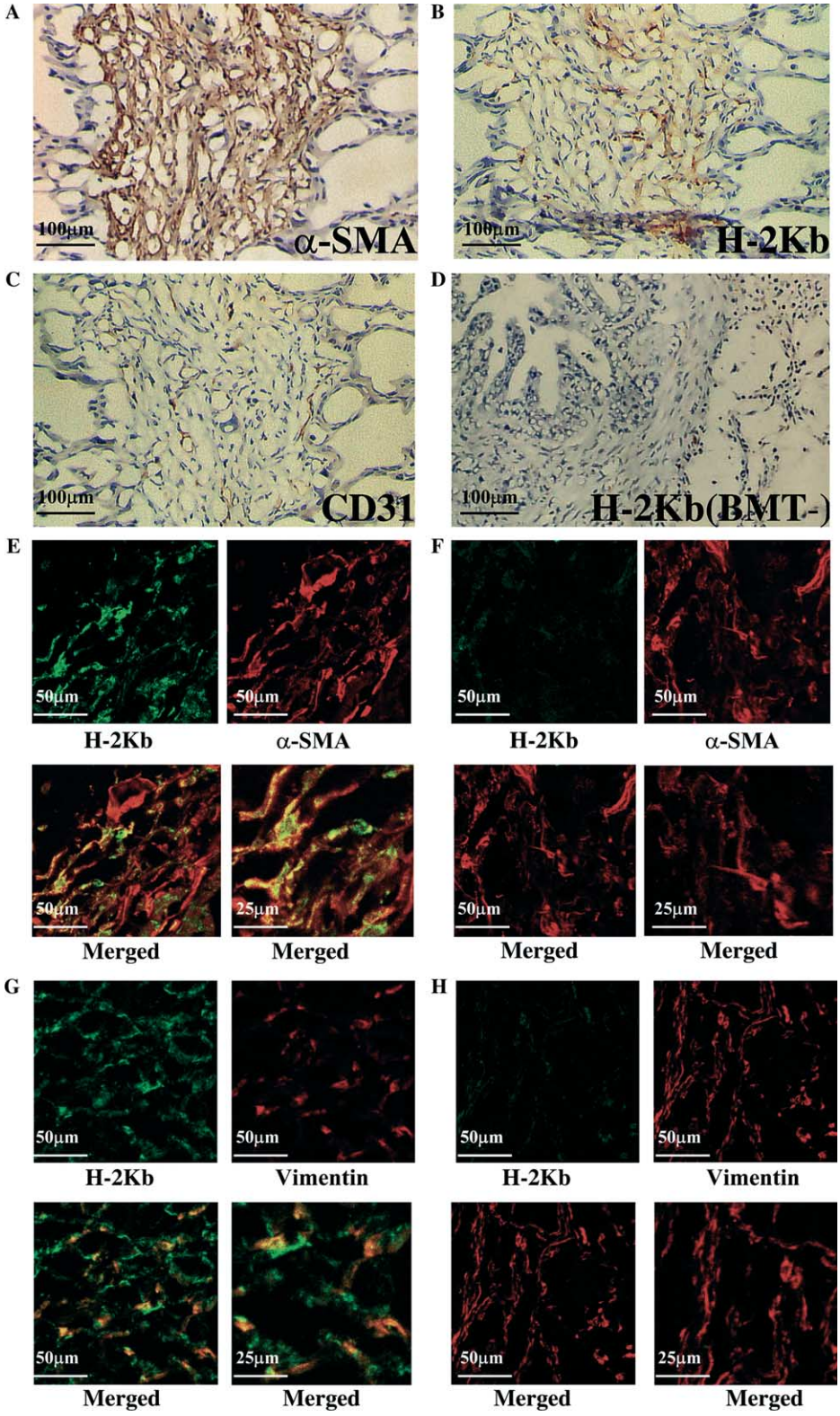

Fig. 4. Immunohistochemical detection of donor-BM-derived cells. α-SMA (A), H-2Kb (B), and CD31 (C) staining of serial sections of desmoplastic stroma. No cells in resected tumors without BMT were positive for anti-H-2Kb (D). (E–F) Colocalization of α-SMA and H-2Kb on spindle cells in the cancer-induced stroma. The upper left panel shows cells immunostained with anti-H-2Kb antibody. The upper right panel shows α-SMA fluorescence in the same area. The lower left panel shows a composite of both fluorophores. The lower right panel shows a higher power view of the same area. (G–H) Colocalization of vimentin and H-2Kb on spindle cells in the cancer-induced stroma. The upper left panel shows cells immunostained with anti-H-2Kb antibody. The upper right panel shows vimentin fluorescence in the same area. The lower left panel shows a composite of both fluorophores. The lower right panel shows a higher power view of the same area.

X-gal-positive (Fig. 3D). Spindle cells that were unassociated with vasculature and reacted positively for X-gal staining were also observed (Figs. 3E and F). Spindle cells in disarray fashion within and around the cancer nests appeared to be activated myofibroblasts and were both α-SMA and X-gal positive (Figs. 3G and H). We used an antibody specific for mouse H-2Kb to further investigate whether these myofibroblasts were of BM origin and found that immunohistochemical detection of H-2Kb seemed to be more sensitive than X-gal staining and equally specific. Although, we were unable to detect any cells positive for anti-H-2Kb within the resected tumor of the SCID mice in the absence of BMT (Fig. 4D), many cells positive for H-2Kb were detected in the tumor tissue when BMT had been performed. Figs. 4A–C show the results of staining for α-SMA, H-2Kb, and CD31, respectively, in serial sections of desmoplastic stroma. About half of the spindle cells in this area were α-SMA/H-2Kb positive, but negative for CD31. The immunofluorescence study also confirmed the presence of α-SMA/H-2Kb or vimentin/H-2Kb double-positive fibroblasts in the cancer-induced stroma (Figs. 4E–H). These results indicate that myofibroblasts of donor BM origin were incorporated into the cancer-induced stroma.

Contribution of BM-derived myofibroblasts to the stromal reaction in the early and late phase of tumor development

In order to analyze how the donor BM-derived myofibroblasts contribute to the stromal reaction in early and late phase of tumor development, we examined the state of the BM-derived myofibroblasts in the resected tumors on days 14 and 28 after subcutaneous Capan-1 xenotransplantation. The average volume of the tumors on days 14 and 28 was 53.3 ± 31.0 and $456.9 \pm 320.9\,mm^3$, respectively. On day 14, small vessels were observed mainly around the cancer nests and the frequency of CD31/H-2kb double-positive cells (BM-derived endothelial cell) was $25.3 \pm 4.4\%$. Myofibroblasts were also mainly seen around the cancer nests and only a small proportion of myofibroblasts ($12.7 \pm 9.6\%$) was α-SMA/H-2Kb double-positive (BM-derived myofibroblast) (Figs. 5A and B). Tumors resected on day 28 showed strong stromal reaction both within and around the cancer nests, which resembled desmoplastic stroma usually seen in human invasive cancer. At this stage, the average proportion of CD31/H-2Kb double-positive cells was $26.7 \pm 9.7\%$ ($n = 4$). On the contrary, the average proportion of α-SMA/H-2Kb double-positive cells had increased to $39.8 \pm 17.1\%$ ($n = 4$) (Fig. 6A). Myofibroblasts adjacent to the cancer nests were H-2Kb negative when examined in serial sections, indicating that they were non-BM-derived myofibroblasts. On the contrary, most myofibroblasts on the outside of H-2Kb negative myofibroblasts were H-2Kb positive (Figs. 5C and D). These findings suggest that donor-BM-derived myofibroblasts were incorporated into the cancer stroma mainly in the late stage (day 28) of cancer development. The proliferative activity of the myofibroblasts in the stroma was analyzed by calculating the Topoisomerase IIα positive ratio, $2.2 \pm 1.2\%$ of the H-2Kb-

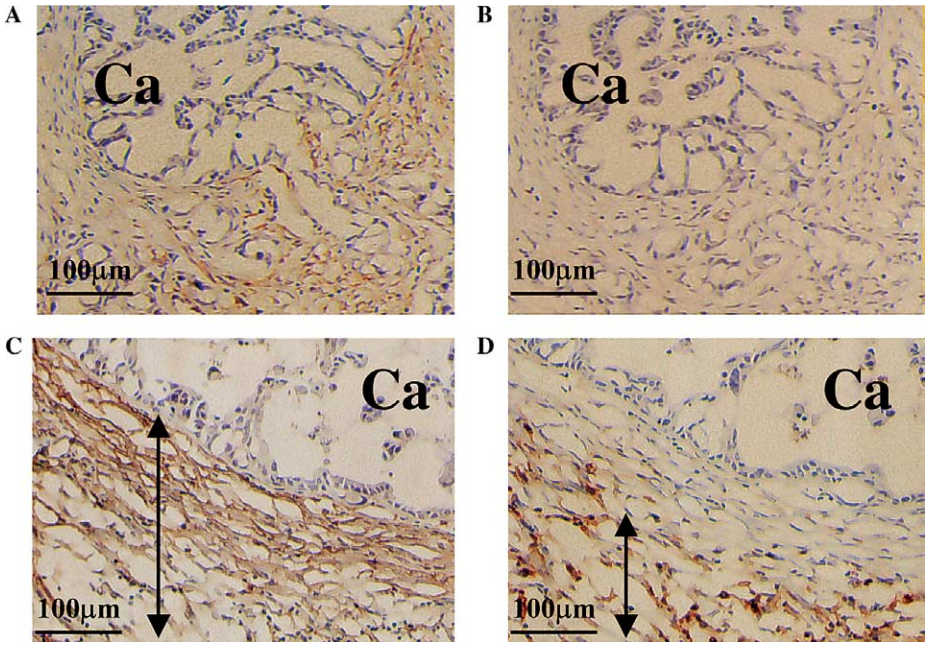

Fig. 5. BM-derived myofibroblasts in the resected Capan-1 on days 14 and 28 after xenotransplantation. α-SMA (A) and H-2Kb (B) staining results in serial sections 14 days after xenografting. Few myofibroblasts in resected tumors are positive for anti-H-2Kb. α-SMA (C) and H-2Kb (D) staining results in serial sections 28 days after xenografting. Myofibroblasts adjacent to the cancer nests were H-2Kb negative. On the contrary, most myofibroblasts on the outside of H-2Kb negative myofibroblasts were H-2Kb positive.

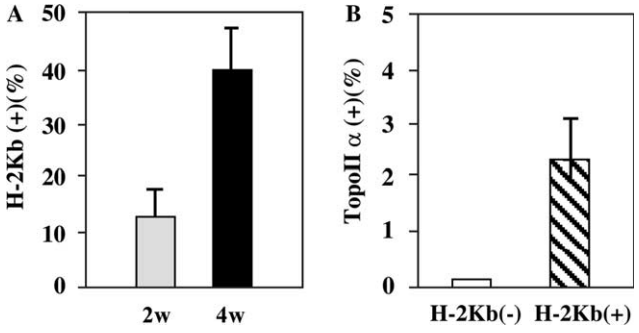

Fig. 6. (A) Percentage of H-2Kb positive myofibroblasts among 500 myofibroblasts in serial sections. Values are means of data from four experiments. *Bars*, SE. (B) Percentage of nuclear topoisomerase IIα positive myofibroblasts among 500 H-2Kb positive and negative myofibroblasts in serial sections. Values are means of data from four experiments. *Bars*, SE.

positive myofibroblasts were found to be as opposed to only $0.3 \pm 0.4\%$ of H-2Kb-negative myofibroblasts (Fig. 6B) and significant proliferative activity was observed in the BM-derived myofibroblasts ($P < 0.05$).

Discussion

The pathogenesis of the stromal reaction in human cancer has remained unclear because of the lack of a good animal model. The main outcome of our study was the establishment of a SCID mouse model that can be used to analyze the stromal response to invading human cancer cells. We used human pancreatic cancer cell line Capan-1 from the following reasons. First, almost all mouse cancer cell lines show solid growth and only quite a little stroma was seen in these cancers when transplanted into immunodeficient mouse, thus evaluating that the pathogenesis of cancer-induced stroma is unsuitable. Second, we examined cancer-induced stroma using various human cancer cell lines and found that stroma generated by Capan-1 resembled human desmoplastic stroma when transplanted into SCID mice. Because of evidences that fibroblasts are heterogeneous in regard to proliferative activity and synthesis of extracellular matrix in the presence of pathological fibrosis [6,7,11–17,21], we hypothesized that the origin of fibroblasts in cancer-induced stroma was also heterogeneous. To test this hypothesis, we used SCID recipients reconstituted with marrow cells from β-gal Tg and RAG-1 deficient double-mutant mice. A small proportion (13%) of H-2Kb/α-SMA double-positive myofibroblasts that were unassociated with CD31-positive cells was observed around the cancer nest 2 weeks after tumor xenotransplantation. These results indicate that a small number of BM-derived myofibroblasts are incorporated into cancer stroma even in the early stage of tumor growth. On the other hand, by 4 weeks after tumor implantation, about 40% of the myofibroblasts in the cancer-induced stroma were of BM origin. Immunohistochemical staining of serial sections revealed that non-BM-derived myofibroblasts exist adjacent to the cancer nest, whereas BM-derived myofibroblasts were on the outside of non-BM-derived myofibroblasts. These data indicated that BM-derived myofibroblasts were incorporated into cancer-induced stroma mainly in the late stage of tumor development. By contrast, the proportion of BM-derived endothelial cells on late phase was almost the same as that on early phase. Taking these results into consideration, it was also deduced that BM-derived myofibroblasts might contribute to the pathogenesis of cancer-induced desmoplastic reaction and might change the "microenvironment" that influences tumor growth. Furthermore, the results of the present study suggest that the local tissue reaction starts at the circumference of a neoplasm in the early stage of tumor development, whereas a remote reaction via the hematopoietic system may act as a regulator of the desmoplastic reaction in the late phase. The BM-derived myofibroblasts in the present study had higher proliferative activity than the non-BM-derived myofibroblasts. In view of this finding and previous reports showing that the proliferative activity of stromal fibroblasts is closely linked to lymph node and distant organ metastasis [6,7], BM-derived myofibroblasts may promote cancer progression. Further analysis is required to elucidate functional differences between BM-derived and non-BM-derived myofibroblasts [22].

The precise origin of myofibroblasts and the molecules involved in their directed migration remains unknown. Several observations have indicated that BM cells exhibit remarkable plasticity and can differentiate into hepatocytes, biliary epithelial cells, endothelial cells, skeletal muscle cells, cardiomyocytes, and neural cells [23–27]. There have been reports suggesting that myofibroblasts can be derived from bone marrow cells [28,29]. Iwano et al. demonstrated that about 15% of bone-marrow-derived myofibroblasts were incorporated into fibrogenic kidney stroma [28]. Our previous study showed that myofibroblasts differentiate from human BM mesenchymal stem cells when exposed to colorectal carcinoma cell lines in vitro [30]. It is possible to speculate that the incorporated myofibroblasts originate from the population of circulating "fibrocytes" that comprise 0.1–0.5% of the human non-erythrocytic cell population in peripheral blood described by Abe et al. [31,32]. Circulating fibrocytes migrate to skin wounds and are smooth muscle actin positive. They express collagens I and III, fibronectin, CD45RO, CD13, and CD34. Moreover, fibrocytes isolated from peripheral blood have been reported to secrete a unique profile of cytokines [33]. Thus it is also possible that fibrocytes derived from BM enter the peripheral blood and migrate to the cancer induced stroma.

In this study, we sublethally irradiated SCID (H2-d) mice and infused them with β-gal Tg RAG-1−/− BM cells (H2-b). Although it seemed plausible that GVHD might artificially influence BM cell contribution to the pathogenesis of cancer induced stromal reaction, we did not find any clear evidence of GVHD effects in a histological examination [34] and did not observe any BM-derived myofibroblasts in non-cancerous subcutaneous tissue, lung, spleen or liver (data not shown). Therefore, our findings demonstrate a specific contribution of BM-derived cells to the cancer induced stroma.

Targeting the tumor microenvironment would increase the treatment effectiveness for cancer [35,36]. Our results raise the possibility of using BM-derived myofibroblast progenitor cells as targets of novel therapies to prevent or slow the local growth of cancer cells. There are advantages to using myofibroblast progenitor cells as targets. First, it is likely that most invasive cancers cause a desmoplastic reaction to some extent, thereby providing a common target for the treatment of many types of cancers. Second, myofibroblasts are normal cells with a low intrinsic mutation rate and therefore are less likely to acquire a drug-resistant phenotype than the genetically unstable cancer cells. A drug delivery system that uses BM-derived myofibroblast progenitor cells would be an attractive means of providing long-term expression of these proteins.

Acknowledgment

We are grateful to Motoko Suzaki for preparing for the manuscript.

References

[1] J.M. Plate, J.E. Harris, Immune cell functions in pancreatic cancer, Semin. Oncol. 29 (2002) 27–30.
[2] J. Folkman, P. Hahnfeldt, L. Hlatky, Cancer: looking outside the genome, Nat. Rev. Mol. Cell Biol. 1 (2000) 76–79.
[3] P. Carmeliet, R.K. Jain, Angiogenesis in cancer and other diseases, Nature 14 (2000) 249–257.
[4] A. Jelaska, D. Strehlow, J.H. Korn, Fibroblast heterogeneity in physiological conditions and fibrotic disease, Springer Semin. Immunopathol. 21 (1999) 385–395.
[5] L. Ronnov-Jessen, B. van Deurs, J.E. Celis, O.W. Petersen, Smooth muscle differentiation in cultured human breast gland stromal cells, Lab. Invest. 63 (1990) 532–543.
[6] T. Hasebe, S. Imoto, T. Ogura, K. Mukai, Proliferative activity of intratumoral fibroblasts is closely correlated with lymph node and distant organ metastases of invasive ductal carcinoma of the breast, Am. J. Pathol. 156 (2000) 1701–1710.
[7] T. Hasebe, S. Sasaki, S. Imoto, A. Ochiai, Highly proliferative fibroblasts forming fibrotic focus govern metastasis of invasive ductal carcinoma of the breast, Mod. Pathol. 14 (2001) 325–337.
[8] Y. Okusa, T. Ichikura, H. Mochizuki, Prognostic impact of stromal cell-derived urokinase-type plasminogen activator in gastric carcinoma, Cancer 85 (1999) 1033–1038.
[9] L.M. Coussens, C.L. Tinkle, D. Hanahan, Z. Werb, MMP-9 supplied by bone marrow-derived cells contributes to skin carcinogenesis, Cell 27 (2000) 481–490.
[10] L.M. Coussens, Z. Werb, Inflammation and cancer, Nature 19–26 (2002) 860–867.
[11] D.M. Garrett, G.W. Conrad, Fibroblast-like cells from embryonic chick cornea, heart, and skin are antigenically distinct, Dev. Biol. 70 (1979) 50–70.
[12] S.L. Schor, A.M. Schor, Clonal heterogeneity in fibroblast phenotype: implications for the control of epithelial–mesenchymal interactions, Bioessays 7 (1987) 200–204.
[13] R.J. Alvarez, M.J. Sun, T.P. Haverty, R.V. Iozzo, J.C. Myers, E.G. Neilson, Biosynthetic and proliferative characteristics of tubulointerstitial fibroblasts probed with paracrine cytokines, Kidney Int. 41 (1992) 14–23.
[14] L. Ronnov-Jessen, B. Van Deurs, M. Nielsen, O.W. Petersen, Identification, paracrine generation, and possible function of human breast carcinoma myofibroblasts in culture, In Vitro Cell Dev. Biol. 28A (1992) 273–283.
[15] L. Ronnov-Jessen, O.W. Petersen, V.E. Koteliansky, M.J. Bissell, The origin of the myofibroblasts in breast cancer. Recapitulation of tumor environment in culture unravels diversity and implicates converted fibroblasts and recruited smooth muscle cells, J. Clin. Invest. 95 (1995) 859–873.
[16] V. Dugina, A. Alexandrova, C. Chaponnier, J. Vasiliev, G. Gabbiani, Rat fibroblasts cultured from various organs exhibit differences in alpha-smooth muscle actin expression, cytoskeletal pattern, and adhesive structure organization, Exp. Cell Res. 238 (1998) 481–490.
[17] O.W. Petersen, H.L. Nielsen, T. Gudjonsson, R. Villadsen, F. Rank, E. Niebuhr, M.J. Bissell, L. Ronnov-Jessen, Epithelial to mesenchymal transition in human breast cancer can provide a nonmalignant stroma, Am. J. Pathol. 162 (2003) 391–402.
[18] B.P. Zambrowicz, A. Imamoto, S. Fiering, L.A. Herzenberg, W.G. Kerr, P. Soriano, Disruption of overlapping transcripts in the ROSA beta geo 26 gene trap strain leads to widespread expression of beta-galactosidase in mouse embryos and hematopoietic cells, Proc. Natl. Acad. Sci. USA 94 (1997) 3789–3794.
[19] P. Mombaerts, J. Iacomini, R.S. Johnson, K. Herrup, S. Tonegawa, V.E. Papaioannou, RAG-1-deficient mice have no mature B and T lymphocytes, Cell 68 (1992) 869–877.
[20] P.P. Tam, M. Parameswaran, S.J. Kinder, R.P. Weinberger, The allocation of epiblast cells to the embryonic heart and other mesodermal lineages: the role of ingression and tissue movement during gastrulation, Development 124 (1997) 1631–1642.
[21] L.A. Kunz-Schughart, P. Heyder, J. Schroeder, R. Knuechel, A heterologous 3-D coculture model of breast tumor cells and fibroblasts to study tumor-associated fibroblast differentiation, Exp. Cell Res. 266 (2001) 74–86.
[22] G.W. Takahashi, D. Moran, D.F. Andrews III, J.W. Singer, Differential expression of collagenase by human fibroblasts and bone marrow stromal cells, Leukemia 8 (1994) 305–308.
[23] Y. Jiang, B.N. Jahagirdar, R.L. Reinhardt, R.E. Schwartz, C.D. Keene, X.R. Ortiz-Gonzalez, M. Reyes, T. Lenvik, T. Lund, M. Blackstad, J. Du, S.A. Aldrich, A. Lisberg, W.C. Low, D.A. Largaespada, C.M. Verfaillie, Pluripotency of mesenchymal stem cells derived from adult marrow, Nature 418 (2002) 41–49.
[24] D.J. Prockop, Marrow stromal cells as stem cells for nonhematopoietic tissues, Science 276 (1997) 71–74.
[25] S.A. Kuznetsov, M.H. Mankani, S. Gronthos, K. Satomura, P. Bianco, P.G. Robey, Circulating skeletal stem cells, J. Cell Biol. 153 (2001) 1133–1140.
[26] D. Lyden, K. Hattori, S. Dias, C. Costa, P. Blaikie, L. Butros, A. Chadburn, B. Heissig, W. Marks, L. Witte, Y. Wu, D. Hicklin, Z. Zhu, N.R. Hackett, R.G. Crystal, M.A. Moore, K.A. Hajjar, K. Manova, R. Benezra, S. Rafii, Impaired recruitment of bone-marrow-derived endothelial and hematopoietic precursor cells

blocks tumor angiogenesis and growth, Nat. Med. 7 (2001) 1194–1201.
[27] S. Makino, K. Fukuda, S. Miyoshi, F. Konishi, H. Kodama, J. Pan, M. Sano, T. Takahashi, S. Hori, H. Abe, J. Hata, A. Umezawa, S. Ogawa, Cardiomyocytes can be generated from marrow stromal cells in vitro, J. Clin. Invest. 103 (1999) 697–705.
[28] M. Iwano, D. Plieth, T.M. Danoff, C. Xue, H. Okada, E.G. Neilson, Evidence that fibroblasts derive from epithelium during tissue fibrosis, J. Clin. Invest. 110 (2002) 341–350.
[29] M. Studeny, F.C. Marini, R.E. Champlin, C. Zompetta, I.J. Fidler, M. Andreeff, Bone marrow-derived mesenchymal stem cells as vehicles for interferon-beta delivery into tumors, Cancer Res. 62 (2002) 3603–3608.
[30] M. Emura, A. Ochiai, M. Horino, W. Arndt, K. Kamino, S. Hirohashi, Development of myofibroblasts from human bone marrow mesenchymal stem cells cocultured with human colon carcinoma cells and TGF beta 1, In Vitro Cell Dev. Biol. Anim. 36 (2000) 77–80.
[31] R. Bucala, L.A. Spiegel, J. Chesney, M. Hogan, A. Cerami, Circulating fibrocytes define a new leukocyte subpopulation that mediates tissue repair, Mol. Med. 1 (1994) 71–81.
[32] R. Abe, S.C. Donnelly, T. Peng, R. Bucala, C.N. Metz, Peripheral blood fibrocytes: differentiation pathway and migration to wound sites, J. Immunol. 166 (2001) 7556–7562.
[33] J. Chesney, C. Metz, A.B. Stavitsky, M. Bacher, R. Bucala, Regulated production of type I collagen and inflammatory cytokines by peripheral blood fibrocytes, J. Immunol. 160 (1998) 419–425.
[34] B.R. Blazar, M. Taylor Brittan, R. McElmurry, L. Tian, A. Panoskaltsis-Mortari, S. Lam, C. Lees, T. Waldschmidt, D.A. Vallera, Engraftment of severe combined immune deficient mice receiving allogeneic bone marrow via in utero or postnatal transfer, Blood 92 (1998) 3949–3959.
[35] M.M. Bilimoria, G.Y. Lauwers, D.A. Doherty, D.M. Nagorney, J. Belghiti, K.A. Do, J.M. Regimbeau, L.M. Ellis, S.A. Curley, I. Ikai, Y. Yamaoka, J.N. Vauthey, Underlying liver disease, not tumor factors, predicts long-term survival after resection of hepatocellular carcinoma, Arch. Surg. 136 (2001) 528–535.
[36] M.J. Bissell, D. Radisky, Putting tumours in context, Nat. Rev. Cancer 1 (2001) 46–54.